Ricardo Almeida Neves Sampayo Ramos

Licenciatura em Micro e Nanotecnologias

Suckerin Protein Colloids used in Drug Delivery Applications

Dissertação para obtenção do Grau de Mestre em Engenharia de Micro e Nanotecnologias

Orientador: Prof. Dr. Ali Gilles Tchenguise Miserez, Professor Auxiliar, School of Materials Science and Engineering, Nanyang Technological University

Co-orientador: Prof. Dr. João Paulo Miranda Ribeiro Borges, Professor Auxiliar, Departamento Ciência dos Materiais, Faculdade de Ciências e Tecnologias da Universidade Nova de Lisboa

Júri:

Presidente: Prof. Dr. João Rodrigo Ferrão Paiva Martins
Arguente(s): Prof. Dr. Pedro Viana Baptista
Vogal(ais): Prof. Dr. João Paulo Miranda Ribeiro Borges

FACULDADE DE CIÊNCIAS E TECNOLOGIA
UNIVERSIDADE NOVA DE LISBOA

Outubro 2015

Jumbo Squid Proteins used in Drug Delivery Applications

Acknowledgements

First I would like to thank Prof. Ali Miserez for giving me the opportunity of doing my master thesis in his lab and for supervising my work.

Quero agradecer também ao Prof. João Paulo Borges pelo apoio que me deu durante a minha tese.

I would like to deeply thank Dr. Ping Yuan for all the support he gave me and for everything he taught me during these 7 months.

Many thanks to Dr. Deepan for all the advices that made my work easier and better.

I want to thank Dawei and Ali B. for teaching me how to express the protein and purify it.

I want to express my gratitude to everyone in BBML for all the help and advices they gave me: Dr. Najmul, Dr. Luigi, Shahrouz, Maryam, Shu Hiew, Jun Jie, Clarinda, Haodong, Cai Hao, Lihong, Akshita and Fu Jing.

I have to thank Ingmar for all his advices and tips that helped me a lot.

Tenho de agradecer aos Amiguinhos, Xoxa, Beast e Susie e à Family, Milho, Diogo (cof cof), Mariana, Sarita e Minima por me aturarem durante este periodo. Um obrigadoao Pepe, à Catarina, Eríca e Carolina pelas grandes conversas que me entreteram bastante. Obrigado também a todos os meus outros amigos que sabem quem são!

Thanks to Oceane, Grant, Ingmar, Tim and Austin for the good environment inside and outside the office and for all the lunches and dinners that made this experience much more memorable.

Finalmente agradeço aos meus pais e avó, pois sem eles nada disto tinha sido possível!

Abstract

This thesis is the first report of suckerin proteins extracted from the sucker ring teeth (SRT) of the Jumbo Squid, being used for drug delivery applications. The main protein used on this work, suckerin-39, was expressed through *E. Coli* cultures and purified with water-based treatments. This protein was processed into particles with average size of 766 nm to be used as carriers for a chemotherapeutic agent, doxorubicin. The particles were chemically cross-linked to increase their stability, and doxorubicin was successfully loaded into these particles that showed controlled released kinetics at different pH. The secondary structure of the particles was determined to be random orientated β-sheet domains and random α-coil domains, and the interaction between the β-sheet and the hydrophobic drug was deemed to be fundamental for a controlled release of doxorubicin. These SRT particles were able to be internalized by HeLa cells, which indicates their great potential as a chemotherapeutic drug carrier for cancer therapy in the future.

Keywords: SRT; suckerin-39; suckerin particles; β-sheet; drug delivery; doxorubicin.

Resumo

Esta tese é a primeira vez que é documentado o uso de proteínas suckerin, extraídas do anel de dentes localizado nas ventosas ao longo dos tentáculos da Lula Jumbo (SRT), em aplicações de libertação de fármacos. A proteína mais utilizada neste trabalho, suckerin-39, foi expressa através de culturas de *E. Coli* e purificada com tratamentos à base de água. Esta proteína foi processada de forma a formar partículas com um tamanho médio de 766 nm para serem utilizadas como veículos para agentes quimió terapeuticos, neste caso doxorubicina. As partículas foram reticuladas quimicamente de forma a aumentar a sua estabilidade e doxorubicina foi encapsulada nas partículas que mostraram uma libertação controlada do fármaco em diferentes pH. A estrutura secundária das partículas foi determinada como sendo domínios de folhas β aleatoriamente ordenados e domínios de hélice α aleatóriamente ordenadas. A interação entre as folhas β e o fármaco na forma hidrofóbica foi considerada como fundamental para a libertação controlada de doxorubicin. As partículas de suckerin foram internalizadas por HeLa cells, o que demonstra um grande potencial como veículo para fármacos no futuro.

Palavras-chave: SRT; suckerin-39; partículas de suckerin; folhas β; libertação de fármacos; doxorubicina.

Units

Da –Dalton

g – Gram

h – Hours

L – Litre

M – Molar

m – Metre

min – Minutes

Pa – Pascal

psi – Pounds per square inch

rpm – Rotation per minute

Abbreviations

Ala – Alanine

ACN – Acetonitrile

AFM – Atomic Force Microscopy

APS – Ammonium Persulfate

CD – Circular Dichroism

DMSO – Dimethyl Sulfoxide

DOX – Doxorrubicin

DTT – Dithiothreitol

EDTA – Ethylenediaminetetraacetic acid

FESEM – Field Emission Scanning Electron Microscopy

Gly – Glycine

His – Histidine

IPTG – Isopropyl β-D-1-thiogalactopyranoside

LB – Luria-Bertani

LEI – Lower Secondary Electron Image

Leu – Leucine

MALDI-TOF – Matrix Assisted Laser Desorption Ionization – Time of Flight

PBS – Phosphate Buffered Saline

PMSF – Phenylmethylsulfonyl Fluoride

Ru(II) – Tris(2,2'-bipyridyl)dichlororuthenium(II) hexahydrate

Ser – Serine

SLS – Static Light Scattering

SRT – Suckerin Ring Teeth

TEA – Triethylamine

TFA – Trifluoroacetic Acid

Thr – Threonine

Tyr – Tyrosine

Val – Valine

Table of Contents

1 Introduction 1

1.1 Motivation 1

1.2 Spider Silk as a Bio-inspired Material 1

1.3 A New Interesting Silk-like Material from the Jumbo Squid 2

1.3.1 Suckerin-39 3

1.4 Recombinant Protein Expression 4

1.5 Protein Crosslinking 4

1.6 Drug Delivery 5

1.6.1 Mechanisms for an Efficient Delivery 6

1.6.2 HeLa Cells 6

2 Methods and Characterization 7

2.1 Proteins Synthesis 7

2.1.1 Expression of Recombinant Suckering Proteins 7

2.1.2 Extraction and Purification 7

2.2 Purity Assays 8

2.2.1 SDS Page (Sodium Dodecyl Sulfate Polyacrilamide Gel Electrophoresis) 8

2.2.2 MALDI-TOF 8

2.3 Suckerin-39 Particle Formation and Crosslinking 9

2.4 Particle Characterization 9

2.5 Drug Loading of suckerin-39 Particles 10

2.6 Drug Release Study 10

2.7 In Vitro Studies 10

3 Results and Discussion 12

3.1 SRT protein expression and purification 12

3.1.1 SDS Page 12

3.1.2 MALDI-TOF analysis of SRT protein 13

3.2 Suckerin-39 Particles 14

3.2.1 Preparation of SRT Particles 14
3.2.2 Particle Characterization 15
3.3 Drug Loading 18
3.4 Drug Release 20
3.5 In-Vitro Studies 22
4 Conclusions and Future Work 23
5 Bibliography 24
6 Supporting Information 27

Table of Figures

Figure 1.1– Dosidicus Gigas and suckerin location 2
Figure 1.2 – Primary structure (a) and secondary structure (b) of the suckerin-19 3
Figure 1.3 – Vector 23a(+) used for recombinant protein expression with *E. coli*. 4
Figure 1.4 –Crosslinking reaction of two tyrosine residues. 5
Figure 1.5 – Targeted drug delivery process 6
Figure 3.1 - SDS-PAGE gel of the suckerin recombinant proteins 12
Figure 3.2 – MALDI-TOF mass spectrum of the suckerin-39 recombinant protein. 13
Figure 3.3 - MADI-TOF mass spectrum of the suckerin-25 recombinant protein 13
Figure 3.4 - Optical microscopy images of suckerin-39 particles 14
Figure 3.5 – FE-SEM images of crosslinked suckerin-39 particles. The white bar represents 1 μm. . 15
Figure 3.6 – Particle size calculated from SEM images (with ImageJ). 15
Figure 3.7- Static Light Scattering of a batch of the suckerin-39 particles. 16
Figure 3.8 – AFM images of suckerin-39 particles: a) Amplitude mode and b) phase mode 17
Figure 3.9 – CD signal of suckerin-39 dissolved in acetic acid (5 mg/mL) and suckerin-39 particles dispersed in water. 17
Figure 3.10 – Differential interference contrast (DIC) images of drug loaded suckerin particles: The scale represents 10 μm. 18
Figure 3.11 – Scheme of the loading mechanism of DOX into suckerin-39 particles. Adapted from. 19
Figure 3.12 - Loading efficiency of different initial concentrations of DOX and difference in concentration of the DOX solution before and after the loading process in the inset. 19
Figure 3.13 - Release study of DOX over a period of 60 hours for pH5 and pH7.4 PBS 20
Figure 3.14 - Illustration of DOX release mechanisms from SRT particles 21
Figure 3.15 – Confocal microscopy images of HeLa cells with internalized SRT particles 22
Figure 6.1a – FE-SEM images of suckerin particles aggregation due to interparticle tyrosine crosslinking (x5000 magnification). 27
Figure 6.2a - AFM image in height mode of suckerin particles used to calculate the two diameters (in red) 28
Figure 6.3 - Differential interference contrast images of suckerin particles left resting for 2 days. 29

List of Tables

Table 1.1 - Comparison between mechanical properties of common silks and biomaterial fibers and tissues commonly used today..... 2
Table 1.2 – Comparison between SRT and silkworm and spider dragline silks properties..... 3

1 Introduction

1.1 Motivation

The development of materials that can keep up with the high demanding technological evolution is one of the biggest concerns for our daily life. Nevertheless, when thinking about a long-term solution, this problem doesn't have a straightforward answer. With the increasing pollution and the shortage of resources on earth, the need for new, sustainable and more creative materials is of great challenge. These materials must be made of abundant elements and have a low impact on the environment at the same time. In addition, they must be commercially viable, which means they have to be cheap, easy to synthesize and have similar or better properties than the materials already available in the market.

The evolution of billions of years allows nature to create amazing materials that the human only recently started to explore. Simple phenomenon like burdock burrs getting stuck in dogs hair (which led to the invention of Velcro by George de Mestral in 1948) and amazing ones like the 200 wing flaps per minute of flies are starting to inspire scientists to create new materials in a field called biomimetic engineering.

The synthetic biomaterials in this field are extracted from nature. A good example is spider silk, one of nature's toughest materials that can even be five times stronger than steel by weight. However, to avoid damaging the environment and hurting animals, other ways to synthesize biomaterials have been explored in the past decades. Genetic and protein engineering are two of the answers scientists found. The introduction of synthetic genes into living organisms which can produce encoded proteins allows the expression of recombinant proteins with high control over their properties. This process brings other advantages since it only uses lower temperature water fermentation processes instead of harsh conditions or toxic chemicals. Nevertheless, the yields of reaction still remain low and some steps of the process in protein engineering can be very expensive. [1]

1.2 Spider Silk as a Bio-inspired Material

Silk has received much attention in the past decades due to its interesting mechanical properties. Orb web weaving spiders appear to use a minimum amount of silk in their webs to catch the prey, and their web needs to stop a fast flying insect almost instantly so that the pray can be successfully trapped. To do so, the web must absorb the energy of the insect without falling apart, which requires a high mechanical strength to prevent insects to escape from the web. Several types of silks from different species of spider have been studied in the past few years. When comparing with the mechanical properties of other materials (**Table 1.1**), silk shows a remarkable combination of toughness, strength and ductility while being a biocompatible material. [2]

Table 1.1 - Comparison between mechanical properties of common silks and biomaterial fibers and tissues commonly used today. [3]

Material	UTS (MPa)	Young Modulus (GPa)	% strain at break
B. mori silk	740	10	20
Nephila clavipes silk	875 - 972	11 - 13	17 – 18
Colagena	0.9 – 7.4	0.0018 – 0.046	24 – 68
PLAb	28 - 50	1.2 – 3.0	2 – 6
Bone	160	20	3
Kevlar (49 fiber)	3600	130	2.7
Synthetic rubber	50	0.001	850

[a] Rat-tail collagen Type I, [b] Polylactic acid with molecular weights ranging from 50,000 to 300,000

These amazing properties greatly inspired researchers to use spider silks as biopolymers in several different applications ranging from hydrogels, capsules and particles for drug and gene delivery, to fibers for textiles, sutures for wound ligation and scaffolds for tissue engineering. Due to the biocompatible features of spider silks, they are largely used in biomedical applications.[4] [5]

1.3 A New Interesting Silk-like Material from the Jumbo Squid

The Jumbo squid, *Dosidicus gigas,* is an extreme aggressive predator from the family *Ommastrephidae* found in the eastern Pacific Ocean at depths between 200 and 700 m. This invertebrate can grow up to 2 m and weight 50 kg. Its eight arms and two tentacles bear hundreds of suckers equipped with sharp teeth with which they capture their prey and push it towards a large and sharp beak.[6]

The Jumbo squid's teeth (**Figure 1.1**), called suckering ring teeth (SRT), have a form of rings with triangular teeth which increase the functionality of the suckers. By increasing the shear forces (created by struggling prey), the jumbo squid is able to break the seal created by the infundibulum of the sucker.

Despite lacking a mineral phase, which is the common microstructural strategy used by nature to create hard tissues, the structures of SRT display impressive mechanical properties. Further studies on finding the origin of the SRT roughness led to the discovery of a family of 21 proteins.[7]

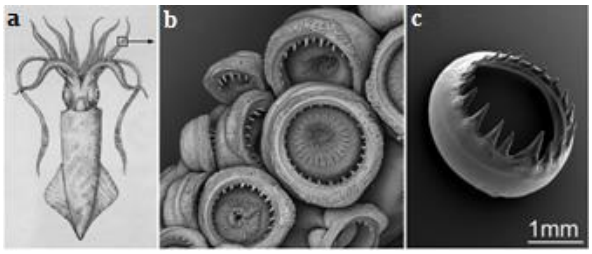

Figure 1.1– Dosidicus Gigas and suckerin location (a), suckerin within the suckers of the squid's tentacles (b) and an isolated suckerin (c). [7]

The similarity between suckerins and silk proteins is appealing given the wide range of biomedical and engineering applications demonstrated for silks, including tissue engineering, drug delivery, and

photonics. Although these two materials have similar mechanical properties, differences between them are summarized in **Table 1.2**. [8]

Table 1.2 – Comparison between SRT and silkworm and spider dragline silks properties. [8]

Properties	SRT	Silkwork and spider dragline silks
Native morphology	bulk	Fiber
Native mechanical loading regime	Tensile, compression - shear	Tensile
Mechanical properties	High E (4.5-8 GPa)	High E (~ 10 GPa)
Structure	β-sheet reinforced network	β-sheet reinforced network
Protein composition	suckerins	Fibroins or spidroins
Molecular Weight	8-50 kDa	Heavy chain silk fibroin, 390 kDa; light chain silk fibroin, 26 kDa; spidroins, 250-300 kDa
Primary amino acid sequence	Ala, Val Thr, Ser, His-rich and Gly, Tyr, Leu-rich modules	Poly(Gly-Ala)/poly-Ala and Gly-rich modules
Ease of full length recombinant protein expression	yes	No
Ease of processing and fabricating materials	Rapid purification, facile water-based fabrication	Harsh solvents often required for fabrication and purification

1.3.1 Suckerin-39

One of the major constituents of the SRT is a protein named suckering-39 that has a molecular weight around 39 kDa. This protein is highly modular exhibiting two alternating domains. One domain contains alanine and histidine rich motifs (around 11 residues), often flanked by proline residues, and the other consists of glycine and tyrosine rich domains (around 20 to 30 residues) which is shown in **Figure 1.2a**. About the secondary structure, it forms randomly orientated β-sheet domains and random α-coil structures (**Figure 1.2b**). [8][9]

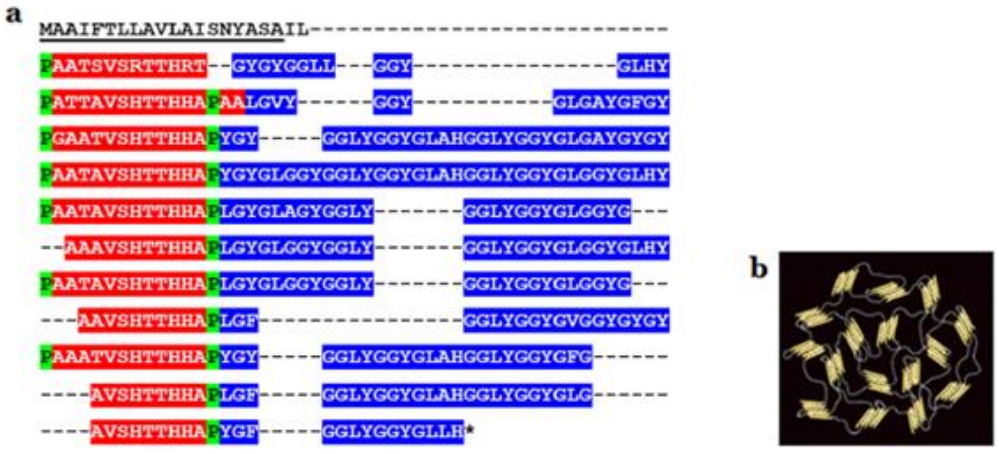

Figure 1.2 – Primary amino acid sequence and repetitive modular organization of the suckerin-39(signal peptide is underlined; Ala, Val, Thr, and His-rich modules are highlighted in red, Gly, Tyr, and Leu-rich modules are in blue, and proline residues are highlighted in green) (a); and secondary structure of the suckerin-19 (b). [8] [9]

1.4 Recombinant Protein Expression

An easy way of reproducing proteins found in nature that doesn't involve the use of harsh conditions and solvents is by using living organisms as a cell factor for expressing recombinant proteins. *Escherichia coli* is one of the most common cell choices for the production of recombinant proteins. [10]

At the theoretical level, there are some important steps needed for obtaining a recombinant protein. A gene of interest is selected and cloned in whatever expression vector is at disposal, then it is transformed into the host of choice, the expression is induced and finally the protein is ready for purification and characterization. [11]

There are several strains of *E. coli* and different vectors that can be used for this purpose. In this project *E. coli* BL21 with the vector PET24 was used to express the suckerin recombinant proteins **Figure 1.3**.

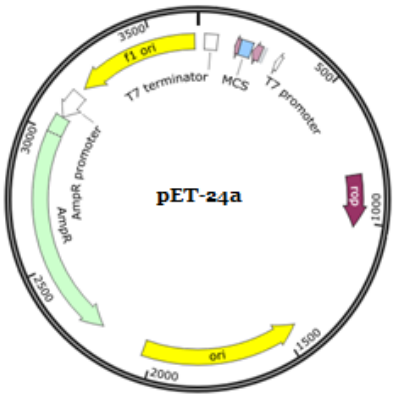

Figure 1.3 – Vector 24a(+) used for recombinant protein expression with *E. coli*.

1.5 Protein Crosslinking

A crosslink is a chemical bond that links one polymer chain to another. This bond can be covalent or ionic and can be used to link proteins together to change their properties. When a biopolymer is crosslinked its ductility decreases and the elastic modulus increases.

In this project, we introduce a non-reversible chemical crosslinking method which was used to stabilize the SRT protein particles. This method is based on the use of a ruthenium complex ($Ru(II)_3^{+2}$) and an electron accepter (ammonium persulfate, APS) to trigger the formation of di-Tyr bonds when the protein is exposed to a light source of 452nm. The ruthenium complex is oxidized by the light to $Ru(III)_3^{+3}$, which is able to remove an electron from the tyrosine residue becoming again $Ru(II)_3^{+2}$. The tyrosine residue lacking an electron forms a covalent bond with another tyrosine residue. The APS is used to receive the free electron generated from the Ru(II) oxidation and prolong the reaction. The process is illustrated in **Figure 1.4**. [12] [13]

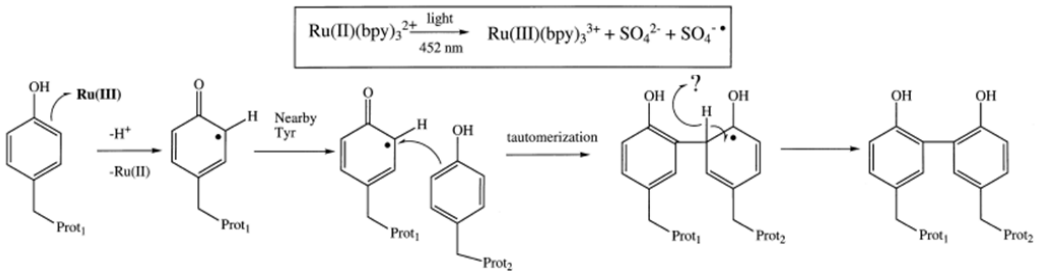

Figure 1.4 –Crosslinking reaction of two tyrosine residues. [12]

1.6 Drug Delivery

In spite of all the advances in medicine and drug development in the past decades, cancer still is one of the leading causes of death in the world. Standard strategies to fight these diseases have side effects that diminish the health of the patients. A common drug used to treat several types of cancer is doxorubicin hydrochloride but this drug is commonly related to severe suppression of haematopoiesis, and gastrointestinal and cardiac toxicity when administered directly in vivo. [14]

In order to enhance the therapeutic outcomes and reduce side effects of anticancer drugs, different types of drug carriers, such as liposomes [15], polymeric micelles[16], polymersomes[17], carbon nanotubes[18], mesoporous silica nanoparticles[19], polymeric nanoparticles[20] and capsules[14] have been extensively studied to improve therapeutic outcomes.

Polymeric nano and microparticles which are biodegradable and biocompatible and can encapsulate an agent of interest into their matrix are of great interest for drug delivery. Due to their sub-cellular size-range they can penetrate deep into tissues through thin capillaries and be internalized by the targeted cells. [21]

Different polymers, both natural and synthetic, have been used to formulate biodegradable micro and nanoparticles. While synthetic polymers have the advantage of sustaining the release of the encapsulated therapeutic agents over longer periods compared to natural polymers, they are often limited by the use of organic solvents and harsher processing conditions.[22]

The suckerin proteins present an excellent profile, which can be potentially explored as a drug delivery vector. Having similar characteristics as spider silks, the suckerins have been proposed as drug delivery vehicles in the current study. These proteins present the advantage of being produced and processed without the use of harsh conditions or solvents. In addition, the suckerin proteins have the advantage of having a high quantity of useful amino acids, like tyrosine and histidine, in its structure opening new possibilities for surface functionalization to optimize targeted delivery of drugs. [8] [13] [23] [24]

1.6.1 Mechanisms for an Efficient Delivery

For the efficient delivery of a therapeutic agent with minimal side effects to the patient from the toxicity of the agent, several critical steps in drug delivery are shown in **Figure 1.5**.

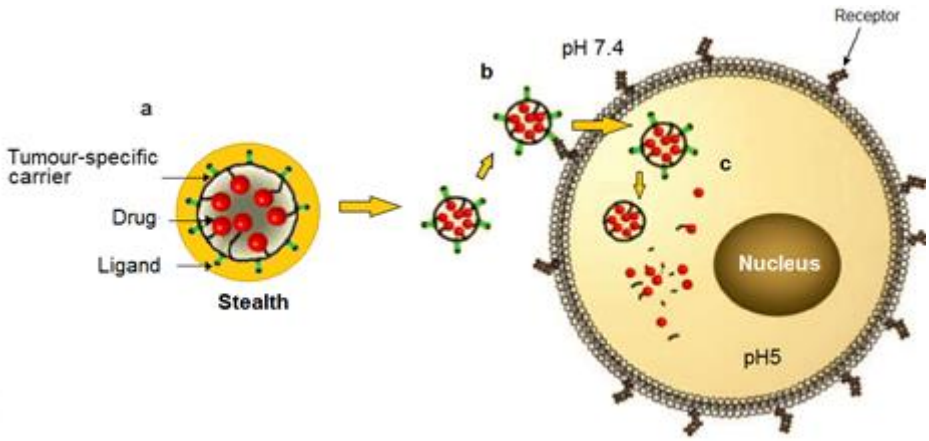

Figure 1.5 – Targeted drug delivery process: a) stealth nanoparticles which is decorated by neutral polymers and targeted ligand over the surface of the nanoparticles ; b) active targeting process where the targeting ligand bind with the receptor through specific ligand-receptor interactions; c) Internalization of targeted nanoparticle by receptor-mediated endocytosis. Adapted from [25]

The first fundamental property of a carrier system should be non-immunogenicity. In another words, the carrier must transport the drug to the targeted tumour tissue without triggering any immune response. When the carrier approaches the targeted tissue, it should be able to recognize and attach to the receptors that are overexpressed by tumour cells in order to facilitate its specific uptake and avoid non-specific uptake by other normal cells. Triggered release can be achieved by pH-sensitive mechanisms in response to an intracellular acidic environment. The pH around tumour tissue is slightly lower than in our circulatory system, which makes it possible to control the release of therapeutic agents by using pH responsive carriers or drugs.[26]

1.6.2 HeLa Cells

HeLa cell is an immortal cancer cell line commonly used in scientific research. They are the oldest and the most used human cell line in scientific research. The cell line was derived from cervical cancer cells and were found to be remarkably durable and prolific. They owe their name to Henrietta Lacks, a patient who died of cancer in 1951, whose HeLa cells were the firsts to be isolated.[27]

2 Methods and Characterization

2.1 Proteins Synthesis

To express the suckerin-39 and suckerin-25 proteins, *E. Coli* BL21(DE3) bacteria containing the recombinant vector *PET-24a* (courtesy of Dr. Shawn Hoon) with the necessary coding were used. These bacteria were stocked at -80 ^{o}C in glycerol. The proteins were expressed, purified and extracted following the protocol described below.

2.1.1 Expression of Recombinant Suckering Proteins

The *E.coli* BL21(DE3) containing pET24a-suckerin-39 or pET24a-suckerin-25 was allowed to grow in LB broth medium (BD, France) in the presence of Ampicillin (Calbiochem, Germany) to attain an OD_{600} between 0.6-0.8 and the target proteins were induced with 1mL of 1 mM IPTG (Gold Biotechnology, USA) and allowed the expression for 7 h. The cells were harvested by centrifugation at 4 x 10^3 rpm for 30 minutes and stored at -70°C until further use.

2.1.2 Extraction and Purification

The cell pellet collected was suspended in 40 mL of lysis buffer (50 mM of Tris at pH7.4, 200 mM of NaCl (Merck, Germany) and 1 mM of PMSF (Sigma Aldrich, USA)), followed by cell disruption with a Microfluidizer (*Microfluidics M110-P*) high-pressure homogenizer (25 kpsi) for six times. PMSF is used to prevent the proteins from being degraded by enzymes. The cell-disrupted samples were subjected to centrifugation at 19 x 10^3 rpm at 4^{o}C for 30 min. The supernatant was discarded and the cell pellet was washed twice with 40 mL of wash buffer I (2% Triton X-100 (Bio-Rad, USA), 100 mM of Tris (Bio-Rad, USA) pH7.4, 5 mM EDTA (Bio-Rad, USA), 2 mM urea (Affymetrix, Germany) and 5 mM of DTT (Bio-Ras, USA)). Urea is used to solubilize the impurities; triton X-100 is to wash the disrupted membranes and the DDT to inhibit protein degradation by the enzymes. After each wash the solution was centrifuged at 6,45 x 10^3 rpm for 10 min and the supernatant is discarded. After this step, the Triton and Urea were removed by washing the cell pellet twice with 40 mL of wash buffer II (100 mM Tris pH 7.4, 5 mM EDTA and 5 mM DDT). After each wash the solution was centrifuged at 6,45 x 10^3 rpm for 10 min and the supernatant was discarded. The resultant cell pellet was re-solubilized in 40 mL of 5% acetic acid (Schedelco, Singapore) and centrifuged at 19 x 10^3 rpm at 4^{o}C for 30 mins. The supernatant was collected and pellet discarded. The solution was dialyzed against 5% acetic acid for 48 hours and then the solution was freezed at -80^{o}C overnight before being lyophilized for 48 hours.

2.2 Purity Assays

2.2.1 SDS Page (Sodium Dodecyl Sulfate Polyacrilamide Gel Electrophoresis)

In order to confirm the presence of suckerin proteins and their purity the samples acquired after the freeze-dried step were analysed by SDS Page. This technique is used to separate different proteins based on their migration on a gel, which is affected by their lengths and mass-to-charge ratio.

There are two different parts that compose the gel: the stacking gel (that forms the entrance of the wells and where the samples are loaded) and the running gel (responsible for the process of migration). Both parts were made of a polyacrylamide matrix in which 10% SDS is added together with a stacking or a running buffer.

To build the gel, 200mL of a monomer solution was prepared (58.4 g of acrylamine (Bio-Rad, USA) and 1.6 g of bis acrilamine (Bio-Rad, USA)) as well as 200 mL of running buffer (36.3 g of Tris pH8.8) and 200 mL of stacking buffer (3 g of Tris pH6.8). For making the preparation of the gel less complicated it was prepared a total of both parts enough for running 5 different gels. The running gel preparation consisted in mixing 5 mL of monomer solution, 3.75 mL of running buffer, 6 mL of milliQ water, 150 µL of 10% SDS, 75 µL of 10% APS (Sigma Aldrich, USA) and 10µL of TEMED (Bio-Rad, USA). For the stacking gel 665 µL of monomer solution, 1.25 mL of stacking buffer, 3 mL of milliQ water, 50 µL of 10% SDS, 25 µL of 10% APS and 2.5 µL of TEMED were mixed. The gel was stacked between two glass plates with a plastic mould with a shape of the wells and left resting for crosslinking. Meanwhile 5 µL of the sample to be analysed was mixed with a loading buffer (4.75 µL of laemmli sample buffer and 0.25 µL of β-mercaptoethanol (Sigma Aldrich, USA)) and heated in a hot water bath for 5 min.

After the gel got crosslinked the sample was loaded in the wells together with a reference buffer and electrophoresis was performed at 0.01 mA for approximately 1h. The resulting gel was stained for 2h in a bath of staining solution (0.165% comassie blue R-250 (Applichem, Germany), 50% methanol (Fisher Scientific), 10% acetic acid) followed by a distaining step overnight in a bath of distaining solution (7% acetic acid an 5% methanol).

2.2.2 MALDI-TOF

The molecular weight of the suckerin proteins expressed previously was determined by MALDI-TOF. A sample was prepared by mixing a 2 µL solution of 1 mg/mL suckerin-39 in 5% acetic acid with a matrix (10 mg/ml of sinapic acid (Sigma Aldrich, USA) dissolved in 50% ACN (FullTime, China) with 1% TFA (Sigma Aldrich, USA)). The spectra was recorded in a *MALDI Shimatsu AXIMA* in linear mode with 100 shots per sample and a power level of 120.

2.3 Suckerin-39 Particle Formation and Crosslinking

For the preparation of particles 120 μL of a 1,33 mg/mL suckerin-39 dissolved in 5% acetic acid was added to 720 μL of a 220 mM NaCl solution. The mixture was votexed for 2 minutes and the particles were observed with an optical microscope (Zeiss Axio Scope.A1). All of the particles were formed by adding the protein to the salt.

The suckerin-39 particles synthetized previously were crosslinked by adding 21.4 μL of 50 mM APS and 53,4 μL of 4 mM Tris(2,2'-bipyridyl)dichlororuthenium(II) hexahydrate (Sigma Aldrich, USA) and exposing the mixture twice to visible light *for 3 min* (using a *Philips QVF135 Halolite* lamp) with 1h interval between the exposures. During and between the exposures the solution was kept stirring at 1×10^3 rpm.

To wash away the Ru(II), the NaCl and the APS the particles were washed 3 times and suspended in clean milliQwater. Finally they were observed under the same optical microscope to check if there was aggregation.

2.4 Particle Characterization

For characterizing the size distribution of the particles, a sample was prepared following the protocol previously presented and analysed with a Particle Size Analyzer LA-960.

To analyse the morphology and topography of the particles, Atomic Force Microscopy and Field Effect Scanning Electron Microscopy were carried out. Both techniques allowed the observation of the shape and roughness of the samples.

For the topographical characterization, AFM data were acquired using an Asylum Research Cypher S. All measurements were performed in tapping mode TM under ambient conditions and the samples were left drying in a mica substrate overnight before being analysed. Commercial soft tapping mode etched silicon probes (NCSTR-20) from Nano World were used.

Scanning electron microscopy images of the protein particles were acquired with a JEOL 7600F FESEM, LEI SEM detector mode and scanning wide distance of 15 mm. The images were taken in the in-lens mode with an acceleration voltage of 5.00kV. The particles were coated with a thin platinum layer (approximately 12 nm).

Circular Dichroism analysis was performed to determine the secondary structure of the proteins before and after the formation of the particles. The proteins were dissolved in 5% acetic acid and the particles in 160 mM of NaCl. An Aviv 420 Circular Dichroism Spectrometer was used together with cuvettes with a light path of 0,1 mm and 0,01 mm bought from Hellma Analytics.

2.5 Drug Loading of suckerin-39 Particles

Using the protocol in the section 2.1, solutions of 6 mg of suckerin-39 particles dispersed in 100 μL of milliQ water were prepared to be loaded with Doxorubicin hydrochloride (Santa Cruz Biotechnology, USA).

To remove the HCl group of the DOX and make it hydrophobic, 600 μL of trimethylamine (Alfa Aesar, UK) were added to 2 mg of drug dissolved in 1 mL of 50% DMSO (Cambridge Isotope Laboratories, UK). After 30 seconds the existence of two phases, a transparent phase and a purple phase, could be observed. The transparent one composed by the TEA that removed the HCl group was discarded.

After being treated with TEA, 100 μL of 1.25 μg/μL doxorubicin solution was added to the suckerin-39 solutions and left stirring overnight in the dark. The next morning the particles were washed 3 times and suspended in 200 μL of milliQ water to be taken to a Microplate Reader (InfiniteM200PRO) to check the fluorescent intensity. The 96 wells black plate with clear fat bottom used were bought from Corning.

In order to analyse the loading efficiency of the particles differential interference contrast images were acquired with an Axio Observer Research microscope with a 543 nm laser light. To get 3D images the particles were dispersed in 2,5% Agarose (Bio-Rad, USA) at 50 ^{o}C and the solution was cooled down to form a gel.

2.6 Drug Release Study

Drug release studies were conducted by dispersing 6 mg of suckerin-39 particles in PBS (Sigma Aldrich, USA) solution with pH7.4 and pH5 and left stirring for 60 h. The PBS was removed, stored and replaced for new one 10 times in specific time intervals (10 min, 30 min, 1h, 3h, 6h, 12h, 24h, 36h, 48h and 60h). The stored PBS solutions were analysed with the Microplate reader to calculate the release profile.

2.7 In Vitro Studies

Human cervical carcinoma cell line, HeLa was purchased from ATCC (Rockville, USA) and cultured in Dulbecco's Modified Eagle Medium (DMEM) supplemented with 10% heat-inactivated fetal bovine serum and 2 mM glutamine, within a cell culture incubator maintained at 37 °C, 5% CO_2 and 95% relative humidity.

For cell uptake visualization, HeLa cells were seeded at 2×10^4 cells per well into 8-well Lab-Tek chambered coverglass slides (Thermo Fisher Scientific, Rochester) and allowed to grow for 24 h. Afterwards, cells were incubated with particles for 24 h followed by washing with PBS three times. Cells were first fixed with 4% paraformaldehyde for 15 min at 37 °C, washed with PBS twice and

stained with wheat germ agglutinin (0.25 μg/mL) at room temperature for 10 min, followed by staining with Hoechst 33342 (2 μg/mL) at room temperature for 15 min.

The system was observed using the same Axio Observer Research microscope used in section 2.3.

3 Results and Discussion

3.1 SRT protein expression and purification

3.1.1 SDS Page

Two suckerin proteins were expressed, extracted, and purified in this study. The expressed suckerin proteins had the molecular weight around 37 kDa (suckerin-39) and 23 kDa (suckerin-25) as indicated in **Figure 3.1** by the darker blue band. In **Figure 3.1b** there are three lighter bands between 10 kDa and 15 kDa that represent the co-existence of other proteins besides the desired suckerin-39. For the purification of suckerin-25, the strategy involving sonicating the sample in each washing step was adopted in order to obtain purer protein. The sonication was expected to break the pellet and release the impurities that were attach to the suckerin protein. However, as can be seen in **Figure 3.1a**, it resulted in a less pure protein sample.

In order to get purer suckerin proteins, two strategies including using either His-tag to purify the protein by immobilized metal affinity chromatography (IMAC), or high performance liquid chromatography (HPLC), could be considered. However, HPLC is time-consuming and the yield is generally limited, which is not suitable for industrial manufacture. The His-tag, which is necessary for IMAC, may affect the properties of the protein. As most of the impurities are of low molecular weight, dialysis membranes with a molecular cut-off close to the protein molecular weight were used to remove those low-molecular-weight impurities.

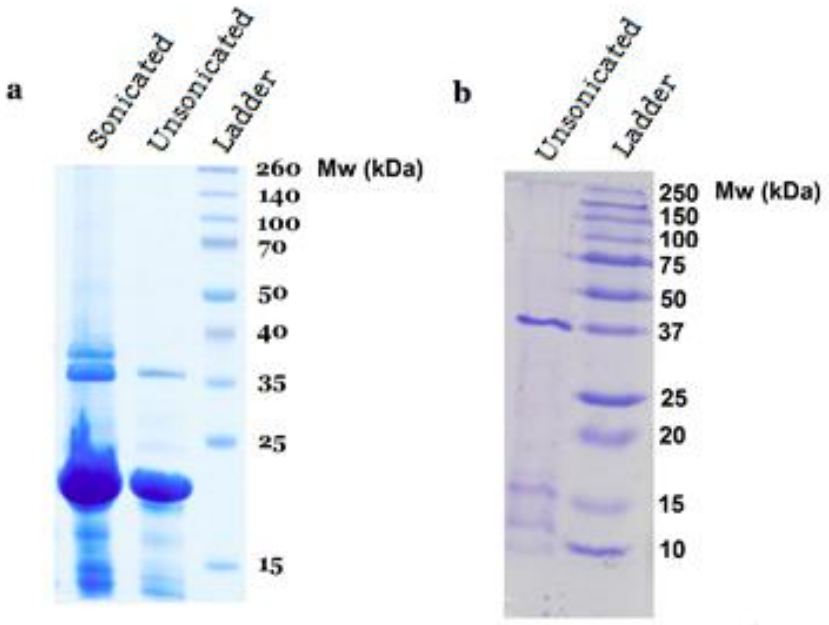

Figure 3.1 - SDS-PAGE gel of the suckerin recombinant proteins: a) suckerin-25 and b) suckerin-39.

3.1.2 MALDI-TOF analysis of SRT protein

As shown in **Figure 3.2** the molecular weight of the suckerin-39 expressed was around 39.8 kDa that is almost identical to the expected value of 39.3 kDa.[8] The peaks at 19.9 kDa, 13.5 kDa and 10.9 kDa are the double charged, triple charged and quadruple charge forms of the protein respectively. The peak at 80.1 kDa corresponds to the dimer (double mass).

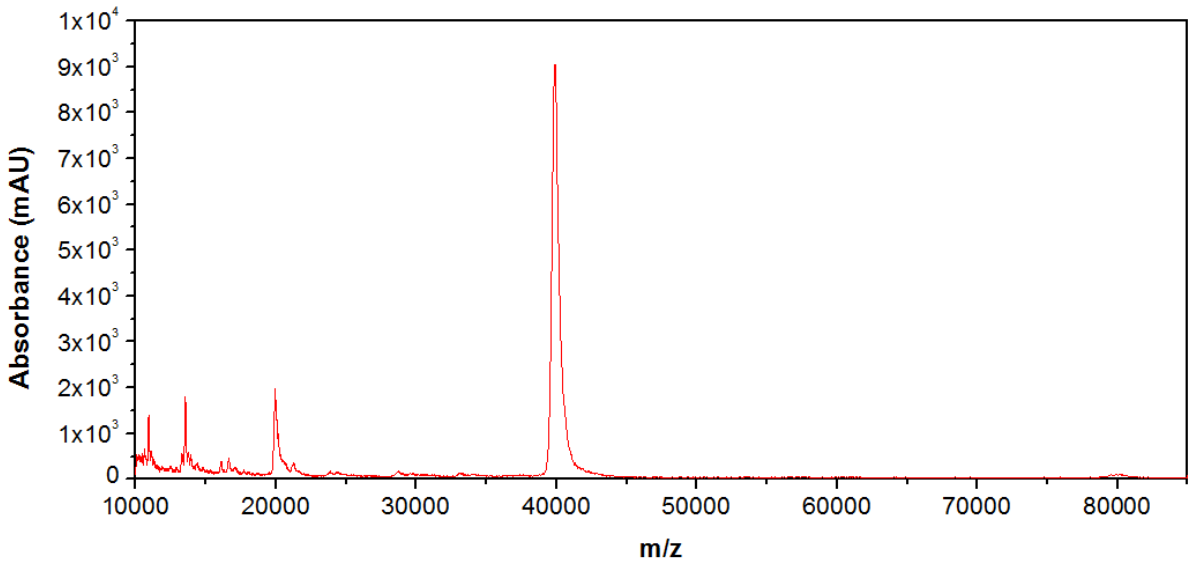

Figure 3.2 – MALDI-TOF mass spectrum of the suckerin-39 recombinant protein.

From the MALDI-TOF signal of the suckerin-25 protein, shown in **Figure 3.3**, the molecular weight of protein expressed was determined to be around 23 kDa. The peaks at 7.6 kDa and 1.5 kDa are the double charged and triple charged forms of the protein respectively. The peak at 46.1 kDa corresponds to the dimer (double mass).

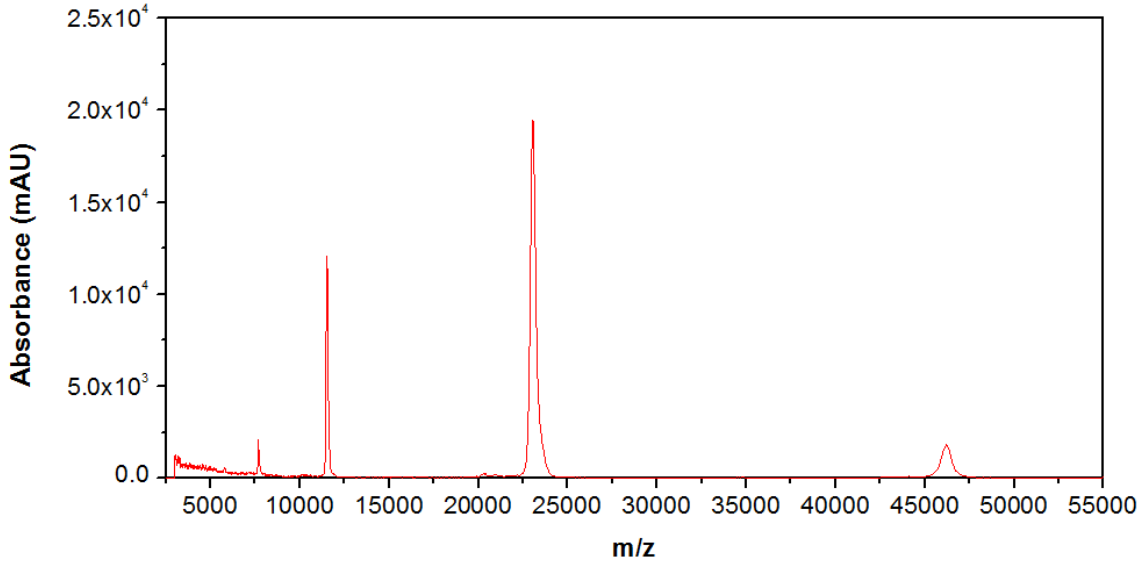

Figure 3.3 - MADI-TOF mass spectrum of the suckerin-25 recombinant protein.

3.2 Suckerin-39 Particles

3.2.1 Preparation of SRT Particles

The suckerin-39 has positively charged, negatively charged and hydrophobic residues in its structure. The positive charges are the main repelling force between the protein chains. When NaCl was added to the solution, the Na+ and Cl- ions shield the charges of the protein and as a result, the hydrophobic residues are able to aggregate forming spherical protein particles due to hydrophobic interactions.

The size of the particles formed could be controlled to some extent by changing the concentration of NaCl. The optical microscopy images (**Figure 3.4**) shows that the suckerin particles prepared in the presence of 166 mM NaCl possess an average sizes around 1 μm, whereas suckerin particles prepared in the presence of 100 mM NaCl presented bigger particle size and higher size distribution.

Higher concentration of salt resulted on protein particles being masked by the ions decreasing the probability of aggregation decreasing the particle size. For lower concentrations the opposite happened with the probability of aggregation being higher increasing the particle size.

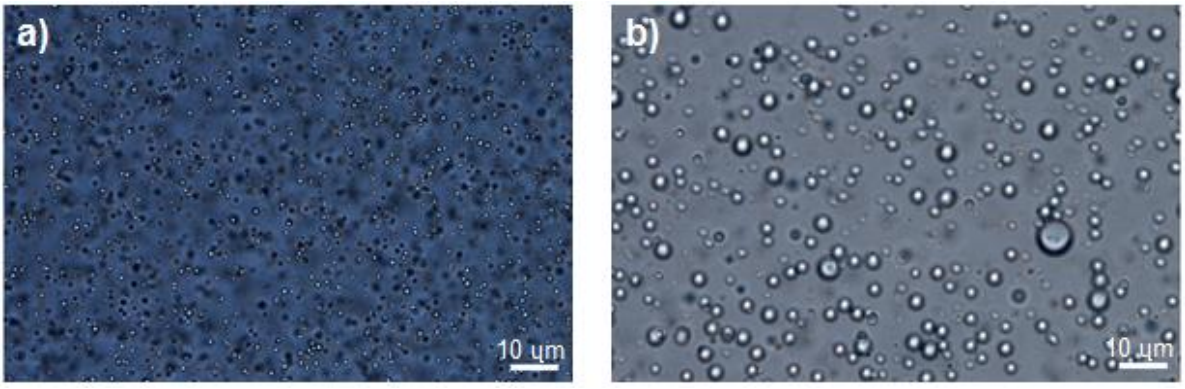

Figure 3.4 - Optical microscopy images of suckerin-39 particles prepared from a) 166mM of NaCl and b) 100mM NaCl. The scale bar represents 10 μm.

All suckerin particles became unstable when NaCl was removed from the solution by washing the particles with DI water. For this reason, it is essential to crosslink the formed particles in order to stabilize them in aqueous conditions.

The particles could be well dispersed in water after crosslinking and could be kept for several days without disassembly at room temperature. Since the crosslinking involves the formation of a covalent bond between two tyrosine residues when the particles were excited with a light source of 285 nm, they are also capable to emit light with wavelength of 400 nm (blue light) [28]. This property may offer a label-free approach for the fluorescence detection of SRT particles.

3.2.2 Particle Characterization

3.2.2.1 Morphology Study of SRT Particles

In this study, FE-SEM was used to characterize the morphology of the suckerin-39 particles. As shown in **Figure 3.5**, the obtained particles are spherical, with an average size of 649 nm (**Figure 3.6**). It was clearly observed that there was no particle aggregation after they were dried (examples of aggregation in supporting information, **Figure 6.1**). The aggregation present was due to interparticle crosslinking, which suggests that the tyrosine of one particle forms a covalent bond with the tyrosine from other particles, instead of forming the covalent bond within the same particle. The aggregation could be avoided by gent stirring while crosslinking the particles.

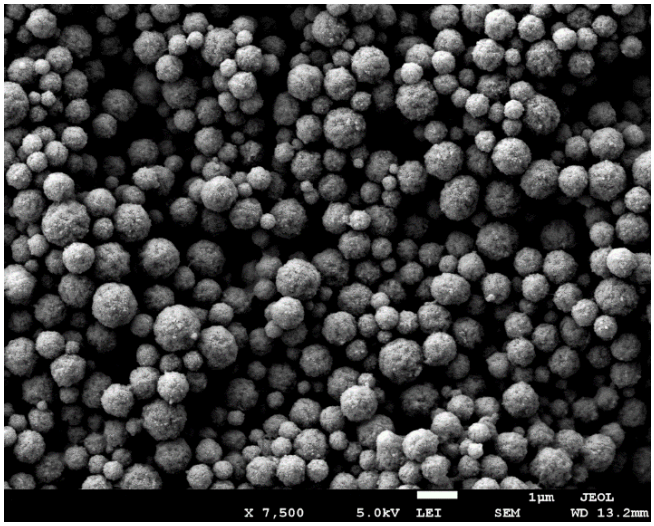

Figure 3.5 – FE-SEM images of crosslinked suckerin-39 particles. The white bar represents 1 µm.

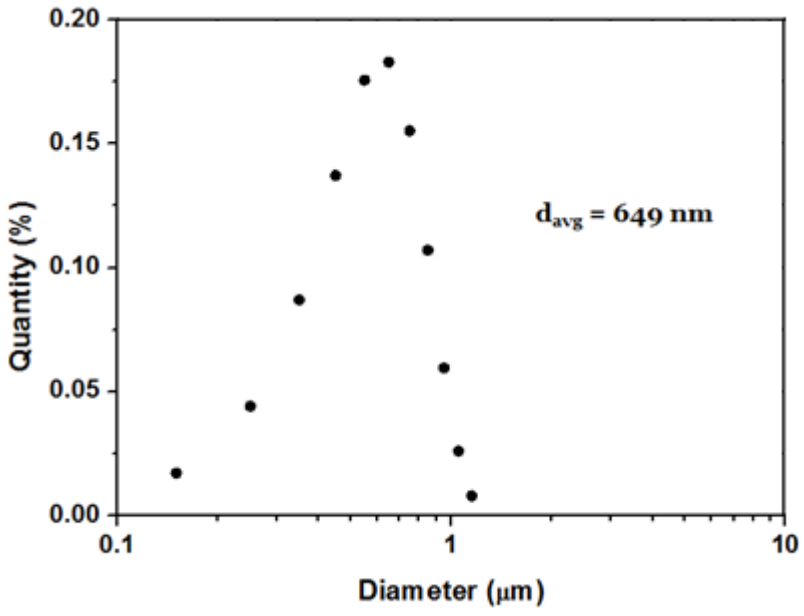

Figure 3.6 – Particle size calculated from SEM images (with ImageJ).

3.2.2.2 SLS Analysis

To check the size distribution, freshly prepared suckerin-39 particles were analysed by SLS. As shown in **Figure 3.7**, the average size of the particles was 766 nm. The average size obtained with SLS is higher than the one from FE-SEM, because the FE-SEM sample was dried before characterization, which probably caused the particles to shrink.

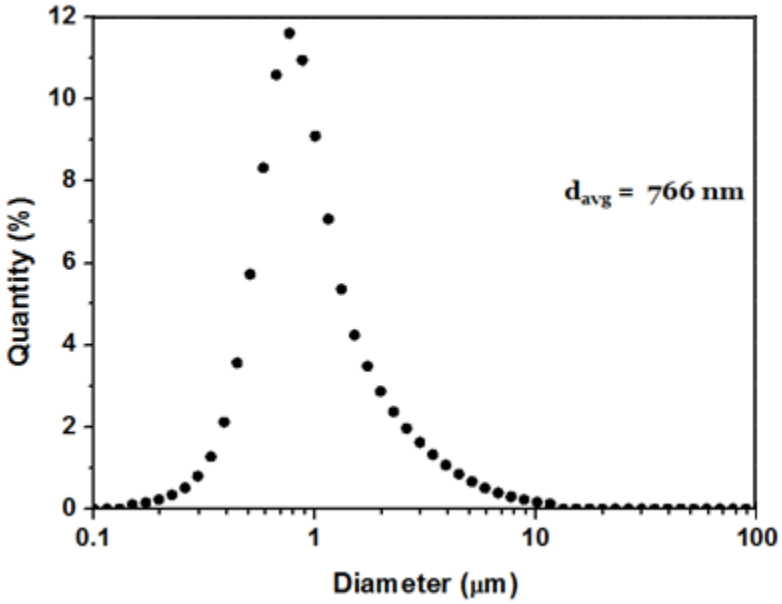

Figure 3.7- Static Light Scattering of a batch of the suckerin-39 particles.

3.2.2.3 AFM Analysis

AFM was also used to characterize the particles and get more information about the particle topography. **Figure 3.8** shows the AFM images of the suckerin-39 particles which are around 1 μm. Since the particles were not spherical, two orthogonal diameters were measured with the height images (supporting information, **Figure 6.1a**). One was 1.1 μm and the other was 1.4 μm. The surface roughness was measured as 32.93 nm, which was determined in a section of the surface of the particle on top (supporting information **Figure 6.1b**). A 3D model was also built based on the data of these measurements (**Figure 6.2c** in the supporting information).

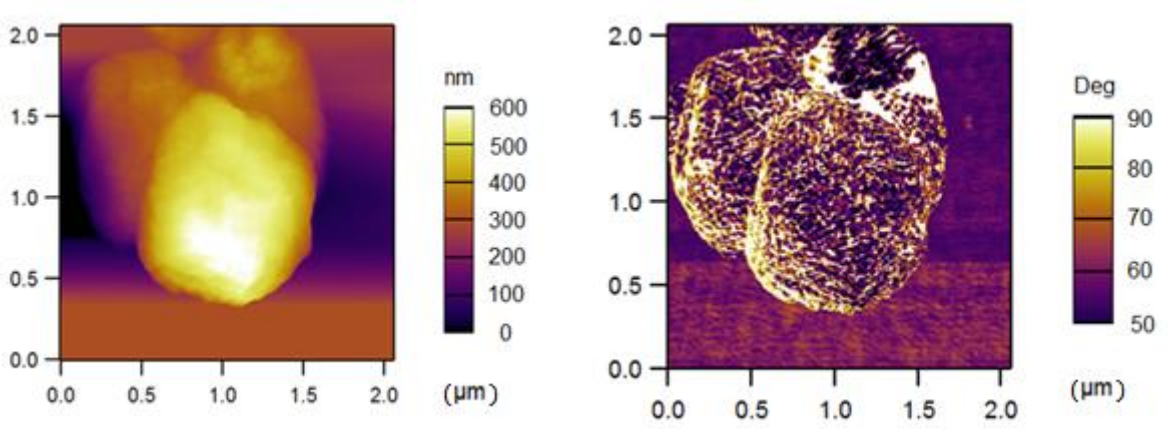

Figure 3.8 – AFM images of suckerin-39 particles: a) Amplitude mode and b) phase mode.

3.2.2.4 Circular Dichroism Analysis

Since the ß-sheet domain of the suckerin-39 particles is hydrophobic, the domain may help to entrap hydrophobic drugs inside the particles through hydrophobic interaction. For this reason, the ß-sheet content of the particles was studied through circular dichroism, as shown in **Figure 3.9**. The difference between the ß-sheet content of the suckerin-39 in solution and in particle form was investigated. For free suckerin-39 in solution, multiple peaks appears in the range of 206-214 nm, which corresponds to ß-sheet structure as reported previously [8]. In the case of suckerin particles, the signal shows an increase in the ß-sheet content as indicated by peak shift to 218 nm. (the interpretation of the results is based on qualitative observations). This reflects the secondary structure content of the suckerin (ß-sheet) changes significantly after the particle formation from free suckerin-39 protein. [8]

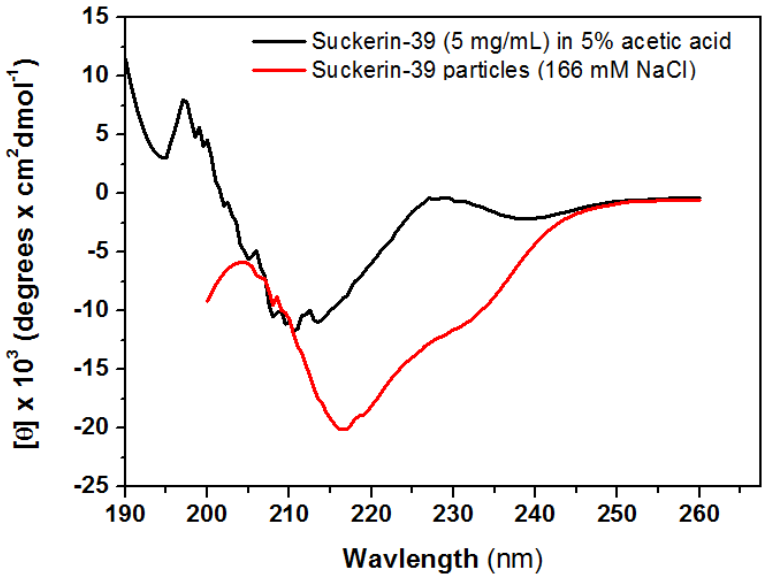

Figure 3.9 – CD signal of suckerin-39 dissolved in acetic acid (5 mg/mL) and suckerin-39 particles dispersed in water.

3.3 Drug Loading

Since DOX became water insoluble after removing its hydrochloride, we used DMSO to dissolve it and expect to load DOX into the β-sheet domain of the suckerin particles. Nevertheless, it was found that DMSO destroyed the suckerin particles in preliminary experiments. As a result, a mixture of DMSO/H_2O was used as solvent for the loading process of DOX to avoid destroying the particles. After loading the drug, fluorescence images of suckerin particles were acquired to check whether DOX loading was successful, since DOX possess inherent red fluorescence. **Figure 3.10** shows the fluorescence and differential interference contrast (DIC) images of suckerin particles where strong red fluorescence, which is generated by DOX inside the particles, could be clearly observed demonstrating that DOX is densely loaded within the particles. As can be seen from Supporting Information (**Figure 6.3**), DOX-loaded particles are still stable with strong red fluorescence after 2 days, and no aggregation was observed during this period, suggesting the good stability of DOX-loaded suckerin particle formulation.

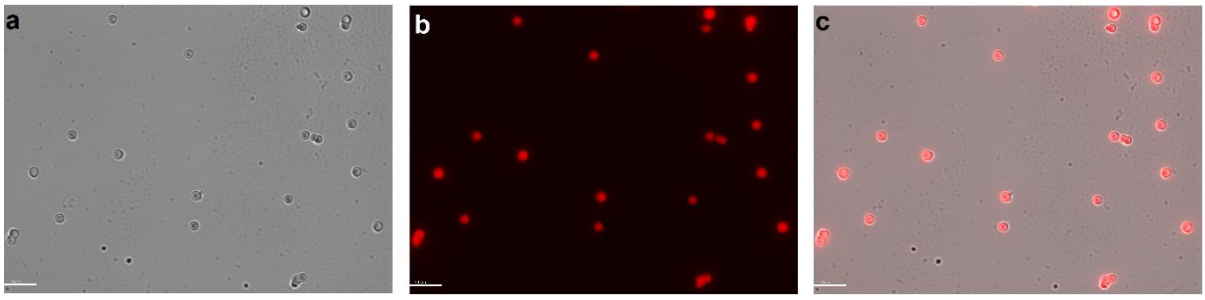

Figure 3.10 – Differential interference contrast (DIC) images of drug loaded suckerin particles: The scale represents 10 μm.

Figure 3.11 illustrates the potential loading mechanism that helps explaining the process how DOX molecules were loaded into the particles. As suckerin particles possess confined β-sheet domains in their backbone, DOX molecules that are dispersed in the solvent can interact with those domains through hydrophobic interactions, especially when a more polar solvent, such as water is introduced to the solution mixture. This study suggests that the confined β-sheet domains of the suckerin particles are able to efficiently encapsulate hydrophobic drugs, which is expected to reduce side effects of DOX for cancer chemotherapy.

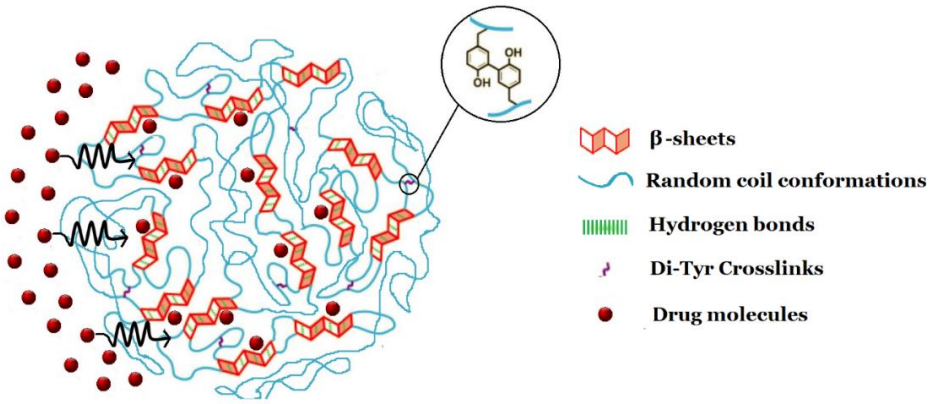

Figure 3.11 – Scheme of the loading mechanism of DOX into suckerin-39 particles. Adapted from [13]

It is also important to optimize the concentration of DOX that is required for the maximum encapsulation efficiency of suckerin particles. To this end, suckerin particles at a fixed concentration were exposed to various concentrations of DOX, and fluorescence intensity of encapsulated drug was measured after removal of the unencapsulated DOX to determine the effective drug loading. As shown in **Figure 3.12a**, the fluorescence intensity increased with the increasing concentration of DOX and stabilized at the DOX concentration of 62.5 µg/µL. Further increase in DOX concentration merely enhanced the DOX fluorescence intensity. **Figure 3.12b** shows the DOX solution before and after mixing with suckerin-39 particles. It was observed that the colour of DOX solution changed significantly after exposure to suckerin particles, which also provide an indirect evidence of successful DOX loading into the particles.

The drug-loaded particles were destroyed to determine the total amount of drug loaded. At DOX concentration of 0.625 µg/µL, the amount of drug loaded was around 575 ng for 6 mg of suckerin particles, which is equivalent to a loading efficiency of 4.6%.

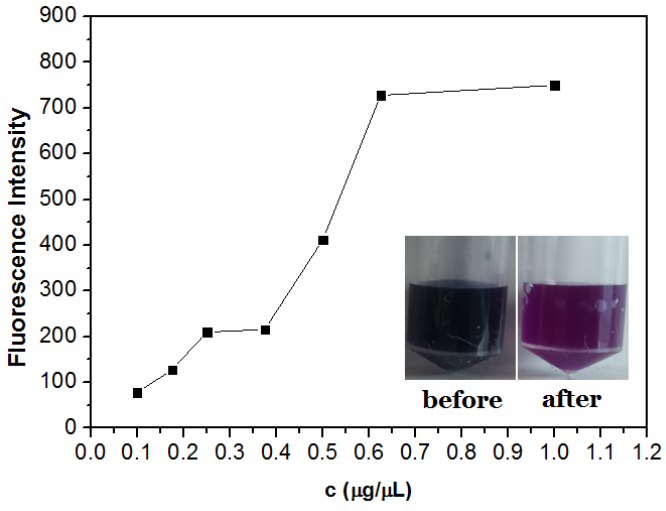

Figure 3.12 - Loading efficiency of different initial concentrations of DOX and difference in concentration of the DOX solution before and after the loading process in the inset.

3.4 Drug Release

The release of DOX from suckerin-39 particles was studied at pH 7.4 and pH 5 (**Figure 3.13**) in order to mimic the physiological and intracellular pH, respectively. At both pH values, the burst release occurred during the first three hours. Afterwards, DOX was gradually released from the particles from 3 to 60 hours. Around 30% of the total encapsulated drug was released at pH 7.4, indicating some leakage of the DOX at extracellular pH and salt concentrations. At pH 5, 85% of the total DOX was released in 60 h. The difference in stability at extracellular physiological pH and intracellular endo/lysosome pH conditions is favourable for the enhanced intracellular release of cargo.[24]

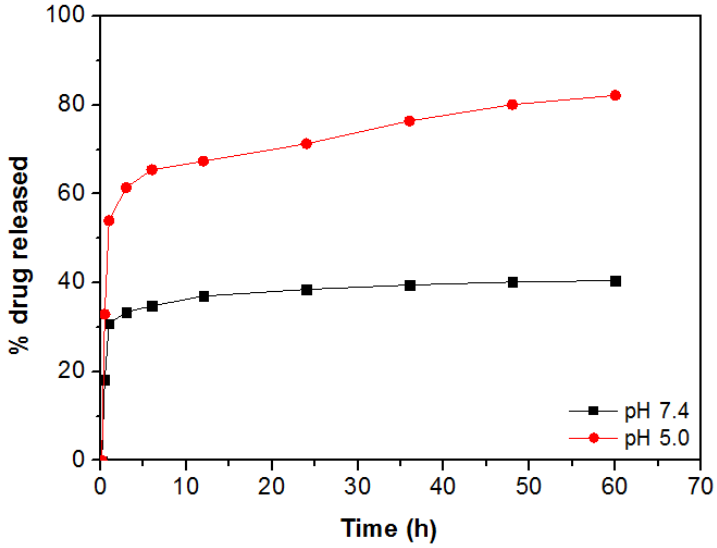

Figure 3.13 - Release study of DOX over a period of 60 hours for pH5 and pH7.4 PBS.

Two mechanisms illustrating the drug release from the suckerin particles are proposed in **Figure 3.14**. DOX is a pH-dependent drug that presents increased hydrophilicity at lower pH, thereby become more positively charged [29]. When the particles are dispersed in PBS at pH 5, DOX becomes more hydrophilic as compared to pH 7.4, and is capable of detaching from the hydrophobic core of the β-sheets and diffusing through the suckerin particles in the salt solution. The histidine residues in the β-sheets also play a fundamental role in the release of the drug. Below pH 6.5, the repelling electrostatic forces between the positively charged histidine moieties (which has pKa around 6.5) and like-charged DOX may push the drugs to the surface of the particles, where they are slowly released to the surrounding environment.

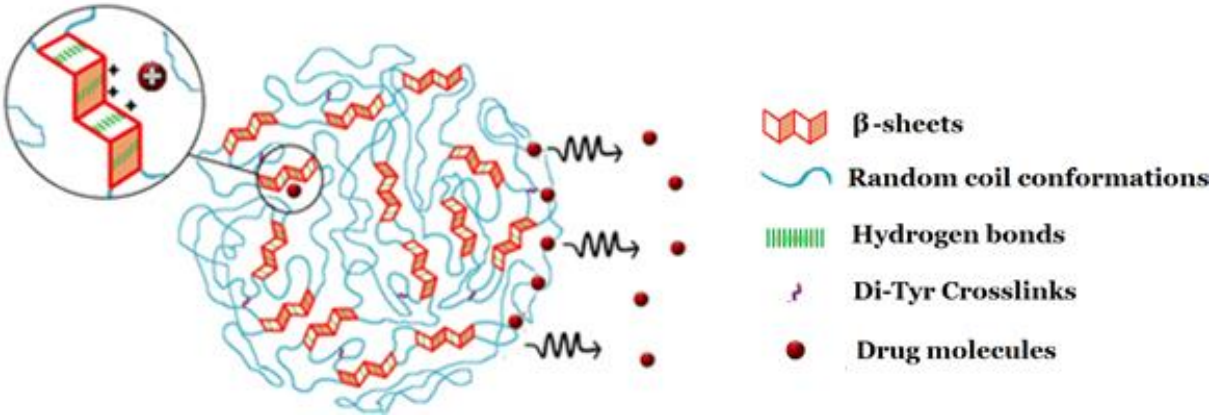

Figure 3.14 - Illustration of DOX release mechanisms from SRT particles. Adapted from [13]

3.6 In-Vitro Studies

As shown in **Figure 3.15a**, the suckerin-39 particles were internalized by HeLa cells after 24 hours of incubation. The intracellular localization of the particles, as shown by 3D reconstructed confocal images, indicates that SRT particles are primarily inside the cell membranes. However, the cell uptake efficiency of suckerin-39 particles was relatively low, probably due to the large size of particles. It is well-documented that particle uptake by cells is size-dependent through endocytosis pathway [30]. Therefore, it is essential to decrease the size of particles in order to increase particle uptake efficiency. In **Figure 3.15c** the particles emit yellow light because the green stain dye reacted with the suckerin particles and the mixture of red (from DOX) and green lights generates yellow.

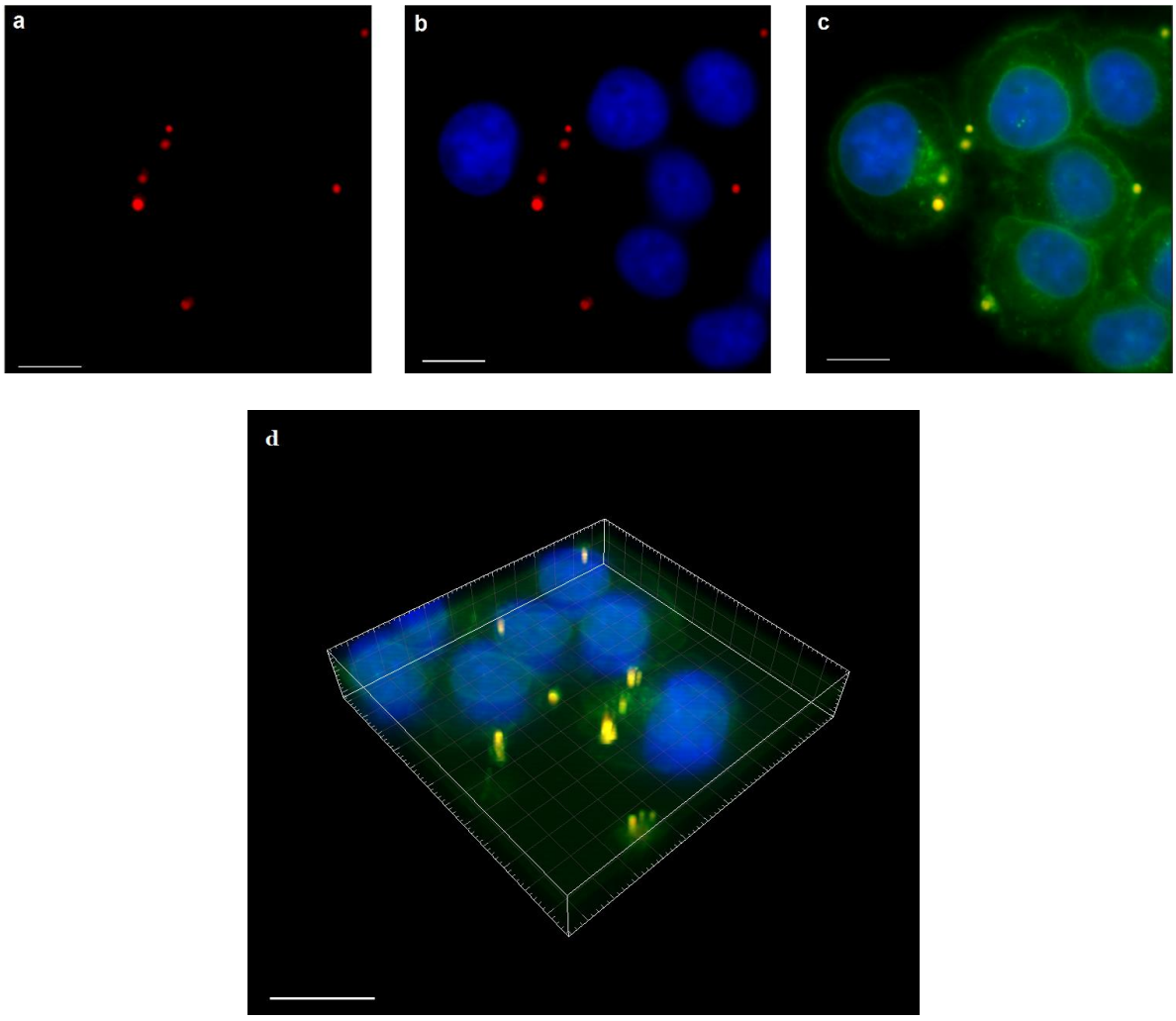

Figure 3.15 – Confocal microscopy images of HeLa cells with internalized SRT particles: a) fluorescence from the DOX (red); b) fluorescence from the DOX (red) and DAPI-stained cell nuclei (blue); c) florescence from the DOX (red), cell nuclei (blue) and cell membranes (green); d) Reconstructed three-dimensional images generated from image (c).

4 Conclusions and Future Work

In this study, the suckerin proteins were successfully expressed with the molecular weight of 23 kDa and 39 kDa. The expressed suckerin proteins showed traces of low molecular impurities in the case of the suckerin-39, and both low and high molecular weight impurities in the case of the suckerin-25. Trying different techniques like salting-out methods or using concentration tubes to separate the impurities from the suckerin proteins might be a good solution for purifying these proteins in the future.

Spherical suckerin-39 particles with an average size of 766 nm were obtained through salt induced protein assembly approach. This method is simple and reproducible, and can produce confined β-sheets domains that are essential for hydrophobic drug encapsulation. Further experiments to reduce particle size down to the nanometre scale is essential in order to increase cell uptake of the particles. Since the suckerin family are composed of multiple suckerin proteins, it might be interesting to explore the particle formation with other suckerin proteins to see whether nanoscaled particles could be obtained.

A crosslinking method was developed to stabilize the particles as well. In the future, it is also important to develop reversible crosslinking methods in order to control the particle degradation at specific conditions. As mentioned, particle degradation is of great importance to reduce side effects of the particles in the human body. In addition, it is fundamental to know if the particles may induce an immunological response in the human body.

High loading efficiency of doxorubicin was achieved without affecting the particles integrity in this study. Investigations on the behaviour of the β-sheet transformation when the particles change from a neutral pH to more acidic conditions should be pursued in order to understand the initial burst of release.

Although particle degradation was observed during the drug release study, this phenomenon was not systemically investigated. Experiments should be planned where the particles are analysed with SLS at different steps of the process to have a better understanding why suckerin particles degrade in spite of stable non-reversible crosslinks within the particles.

Despite the internalization of suckerin particles, cell uptake was low most probably due to their large size. New studies should be performed for longer periods of time to analyse the cell uptake, and the release of the drug at intracellular level as well as the cytotoxicity of these particles.

In the future, suckerin particles could also be functionalized via different protein chemistries for targeted drug delivery. This would provide an important solution to increase the uptake of the suckerin particles as well.

5 Bibliography

[1] J. C. Rodríguez-Cabello, L. Martín, M. Alonso, F. J. Arias, and A. M. Testera, "'Recombinamers' as advanced materials for the post-oil age," *Polymer (Guildf).*, vol. 50, no. 22, pp. 5159–5169, 2009.

[2] J. M. Gosline, P. a Guerette, C. S. Ortlepp, and K. N. Savage, "The mechanical design of spider silks: from fibroin sequence to mechanical function.," *J. Exp. Biol.*, vol. 202, no. Pt 23, pp. 3295–3303, 1999.

[3] G. H. Altman, F. Diaz, C. Jakuba, T. Calabro, R. L. Horan, J. Chen, H. Lu, J. Richmond, and D. L. Kaplan, "Silk-based biomaterials," vol. 24, pp. 401–416, 2003.

[4] J. a. Kluge, O. Rabotyagova, G. G. Leisk, and D. L. Kaplan, "Spider silks and their applications," *Trends Biotechnol.*, vol. 26, no. 5, pp. 244–251, 2008.

[5] F. P. Seib, G. T. Jones, J. Rnjak-Kovacina, Y. Lin, and D. L. Kaplan, "pH-Dependent Anticancer Drug Release from Silk Nanoparticles," *Adv. Healthc. Mater.*, vol. 2, no. 12, pp. 1606–1611, 2013.

[6] R. Rosa and B. a. Seibel, "Metabolic physiology of the Humboldt squid, Dosidicus gigas: Implications for vertical migration in a pronounced oxygen minimum zone," *Prog. Oceanogr.*, vol. 86, no. 1–2, pp. 72–80, 2010.

[7] A. Miserez, J. C. Weaver, P. B. Pedersen, T. Schneeberk, R. T. Hanlon, D. Kisailus, and H. Birkedal, "Microstructural and Biochemical Characterization of the Nanoporous Sucker Rings from Dosidicus gigas," *Adv. Mater.*, vol. 21, no. 4, pp. 401–406, Jan. 2009.

[8] D. Ding, P. a Guerette, S. Hoon, K. W. Kong, T. Cornvik, M. Nilsson, A. Kumar, J. Lescar, and A. Miserez, "Biomimetic production of silk-like recombinant squid sucker ring teeth proteins.," *Biomacromolecules*, vol. 15, no. 9, pp. 3278–89, Sep. 2014.

[9] P. a Guerette, S. Hoon, D. Ding, S. Amini, A. Masic, V. Ravi, B. Venkatesh, J. C. Weaver, and A. Miserez, "Nanoconfined β-sheets mechanically reinforce the supra-biomolecular network of robust squid Sucker Ring Teeth.," *ACS Nano*, vol. 8, no. 7, pp. 7170–9, Jul. 2014.

[10] G. L. Rosano and E. a. Ceccarelli, "Recombinant protein expression in Escherichia coli: Advances and challenges," *Front. Microbiol.*, vol. 5, no. APR, pp. 1–17, 2014.

[11] H. P. Sørensen and K. K. Mortensen, "Advanced genetic strategies for recombinant protein expression in Escherichia coli," *J. Biotechnol.*, vol. 115, no. 2, pp. 113–128, 2005.

[12] D. a Fancy, C. Denison, K. Kim, Y. Xie, T. Holdeman, F. Amini, and T. Kodadek, "Scope,

limitations and mechanistic aspects of the photo-induced cross- linking of proteins by water-soluble metal complexes," *Chem Biol*, vol. 7, no. 9, pp. 697–708., 2000.

[13] D. Ding, P. a. Guerette, J. Fu, L. Zhang, S. a. Irvine, and A. Miserez, "From Soft Self-Healing Gels to Stiff Films in Suckerin-Based Materials Through Modulation of Crosslink Density and β -Sheet Content," *Adv. Mater.*, p. n/a–n/a, 2015.

[14] Y. Ping, J. Guo, H. Ejima, X. Chen, J. J. Richardson, H. Sun, and F. Caruso, "pH-Responsive Capsules Engineered from Metal-Phenolic Networks for Anticancer Drug Delivery," *Small*, p. n/a–n/a, 2015.

[15] T. Lian and R. J. Ho, "Trends and developments in liposome drug delivery systems.," *J. Pharm. Sci.*, vol. 90, no. 6, pp. 667–680, 2001.

[16] H. Sun, B. Guo, R. Cheng, F. Meng, H. Liu, and Z. Zhong, "Biodegradable micelles with sheddable poly(ethylene glycol) shells for triggered intracellular release of doxorubicin," *Biomaterials*, vol. 30, no. 31, pp. 6358–6366, 2009.

[17] J. Xu, Q. Zhao, Y. Jin, and L. Qiu, "High loading of hydrophilic/hydrophobic doxorubicin into polyphosphazene polymersome for breast cancer therapy," *Nanomedicine Nanotechnology, Biol. Med.*, vol. 10, no. 2, pp. 349–358, 2014.

[18] Z. Liu, K. Chen, C. Davis, S. Sherlock, Q. Cao, X. Chen, and H. Dai, "Drug delivery with carbon nanotubes for in vivo cancer treatment," *Cancer Res.*, vol. 68, no. 16, pp. 6652–6660, 2008.

[19] I. I. Slowing, J. L. Vivero-Escoto, C.-W. Wu, and V. S.-Y. Lin, "Mesoporous silica nanoparticles as controlled release drug delivery and gene transfection carriers.," *Adv. Drug Deliv. Rev.*, vol. 60, no. 11, pp. 1278–1288, 2008.

[20] T. Yucel, M. L. Lovett, and D. L. Kaplan, "Silk-based biomaterials for sustained drug delivery," *J. Control. Release*, vol. 190, pp. 381–397, 2014.

[21] J. Panyam and V. Labhasetwar, "Biodegradable nanoparticles for drug and gene delivery to cells and tissue," *Adv. Drug Deliv. Rev.*, vol. 55, no. 3, pp. 329–347, 2003.

[22] S. M. Moghimi, A. C. Hunter, and J. C. Murray, "Long-Circulating and Target-Specific Nanoparticles : Theory to Practice," vol. 53, no. 2, pp. 283–318, 2001.

[23] M. P. Neubauer, C. Blüm, E. Agostini, J. Engert, T. Scheibel, and A. Fery, "Micromechanical characterization of spider silk particles," *Biomater. Sci.*, vol. 1, no. 11, p. 1160, 2013.

[24] A. Lammel, M. Schwab, M. Hofer, G. Winter, and T. Scheibel, "Recombinant spider silk particles as drug delivery vehicles," *Biomaterials*, vol. 32, no. 8, pp. 2233–2240, 2011.

[25] R. Sinha, G. J. Kim, S. Nie, and D. M. Shin, "Nanotechnology in cancer therapeutics: bioconjugated nanoparticles for drug delivery.," *Mol. Cancer Ther.*, vol. 5, no. 8, pp. 1909–1917, 2006.

[26] M. Ding, N. Song, X. He, J. Li, L. Zhou, H. Tan, Q. Fu, and Q. Gu, "Toward the next-generation nanomedicines: Design of multifunctional multiblock polyurethanes for effective cancer treatment," *ACS Nano*, vol. 7, no. 3, pp. 1918–1928, 2013.

[27] R. Rahbari, T. Sheahan, V. Modes, P. Collier, and C. Macfarlane, "Europe PMC Funders Group Europe PMC Funders Author Manuscripts A novel L1 retrotransposon marker for HeLa cell line identification," vol. 46, no. 4, pp. 277–284, 2009.

[28] E. Peña, a. Bernardo, C. Soler, and N. Jouve, "Do tyrosine crosslinks contribute to the formation of the gluten network in common wheat (Triticum aestivum L.) dough?," *J. Cereal Sci.*, vol. 44, no. 2, pp. 144–153, 2006.

[29] C. Sanson, C. Schatz, J. F. Le Meins, A. Soum, J. Thévenot, E. Garanger, and S. Lecommandoux, "A simple method to achieve high doxorubicin loading in biodegradable polymersomes," *J. Control. Release*, vol. 147, no. 3, pp. 428–435, 2010.

[30] S. Zhang, J. Li, G. Lykotrafitis, G. Bao, and S. Suresh, "Size-dependent endocytosis of nanoparticles," *Adv. Mater.*, vol. 21, no. 4, pp. 419–424, 2009.

6 Supporting Information

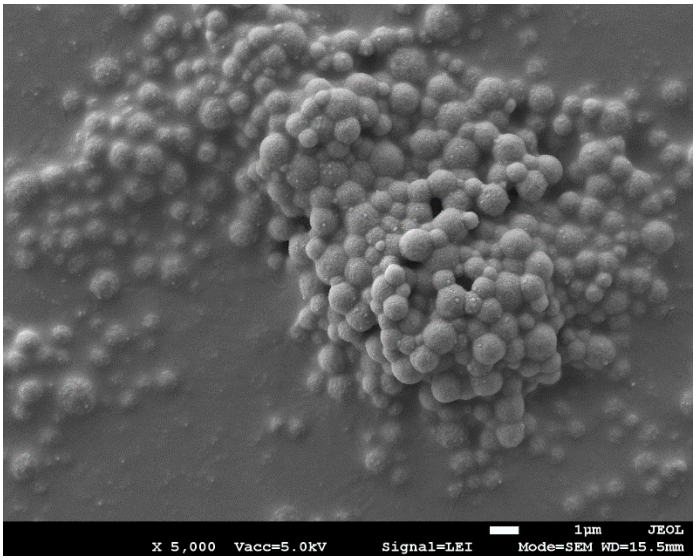

Figure 6.1a – FE-SEM images of suckerin particles aggregation due to interparticle tyrosine crosslinking (x5000 magnification).

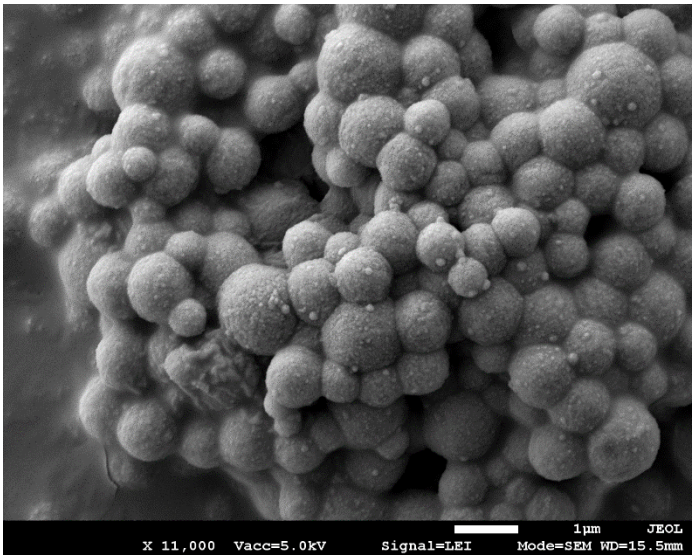

Figure 6.1b – FE-SEM images of suckerin particles aggregation due to interparticle tyrosine crosslinking (x11000 magnification).

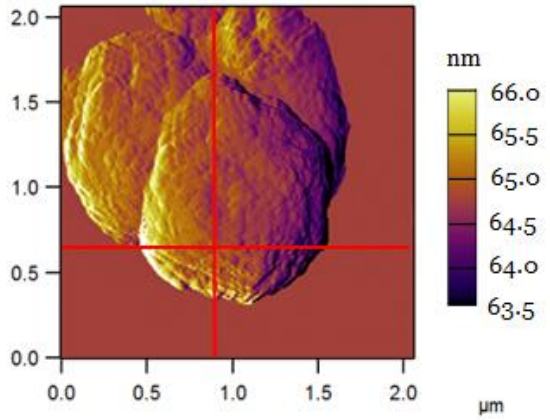

Figure 6.2a - AFM image in height mode of suckerin particles used to calculate the two diameters (in red).

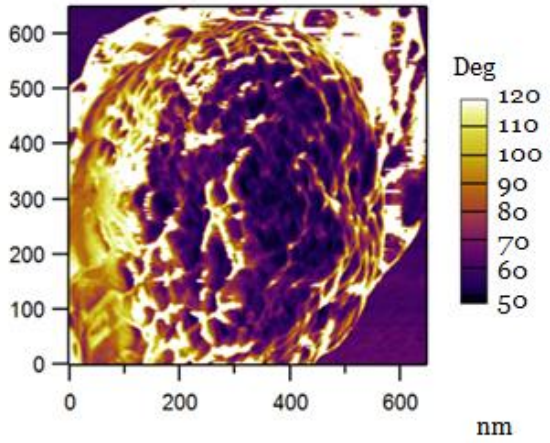

Figure 6.2b - AFM image in phase mode of the section of a suckerin particle used to calculate the surface roughness.

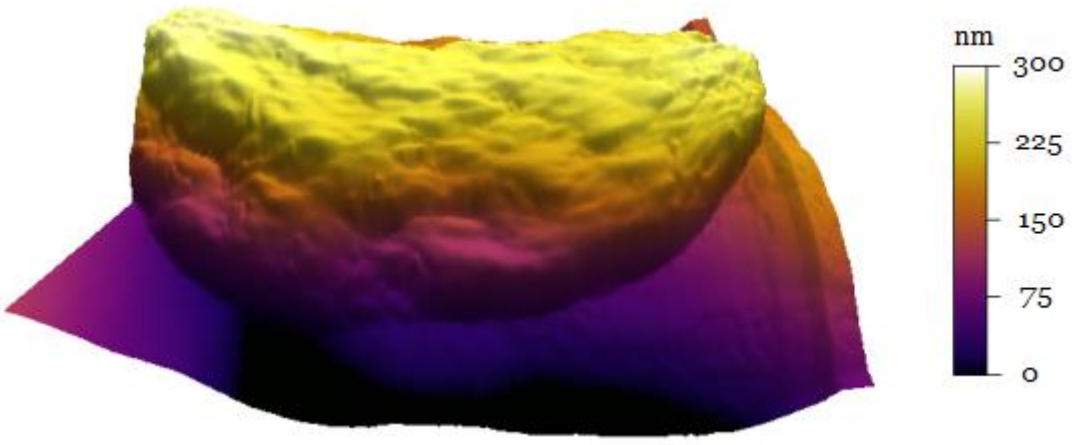

Figure 6.2c - 3D model created with the data from the AFM images of a suckerin particles in dried state.

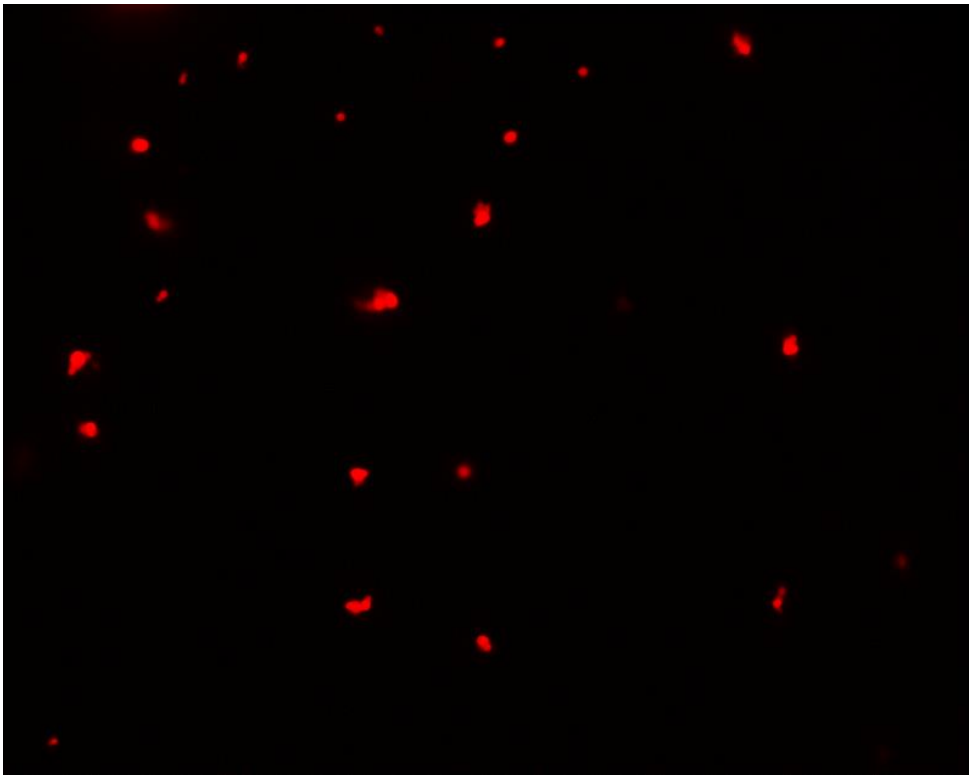

Figure 6.3 - Differential interference contrast images of suckerin particles left resting for 2 days.